

Sub-daily northern hemisphere ionospheric maps using a world-wide network of GPS receivers

Brian D. Wilson, Anthony J. Mannucci, and Charles D. Edwards

Jet Propulsion Laboratory, California Institute of Technology
Pasadena, CA 91109

Ionospheric total electron content (TEC) data derived from dual-frequency Global Positioning System (GPS) signals from 30 globally distributed network sites are fit to a simple ionospheric shell model, yielding a map of the ionosphere in the northern hemisphere every 12 hours during the period of Jan. 1-15, 1993, as well as values for the satellite and receiver instrumental biases. Root-mean-square (≈ 1 MS) residuals of 2-3 TEC units are observed over the 20-80 degree latitude band. Various systematic errors affecting the TEC estimates are discussed. The capability of using these global maps to produce ionospheric calibrations for sites at which no GPS data are available is also investigated.

1 Introduction

Radio signals propagating through the Earth's ionosphere incur a phase advance and group delay proportional to the integrated electron density along the signal raypath. These effects represent a significant error source for a variety of tracking, navigation, radio science, and radio astronomy applications. The Deep Space Network (DSN) is responsible

for navigating spacecraft such as Magellan, Galileo, and Ulysses using single-frequency (S or X band) Doppler and range radio metric data. In order to navigate accurately, the radio metric data must be corrected for the dispersive delay effects of charged particles. Ionospheric calibrations are also required for other purposes such as correcting single-frequency Very Long Baseline Interferometry (VLBI) measurements and for verifying the calibration of the TOPEX dual-frequency altimeter. In the past, the DSN has generated ionospheric calibrations using Faraday rotation data or dual-frequency Global Positioning System (GPS) delay data from a single (on-site) GPS receiver [Lanyi and Roth, 1988]. These single-site techniques provide only limited sky coverage and are sensitive to data gaps.

In order to improve the accuracy of the ionosphere calibrations, the DSN has begun exploiting an existing world-wide network of GPS receivers to produce global maps of vertical total electron content (TEC). The continuously operating International GPS Geodynamics Service (IGS) network had about 30 stations, as of Jan. 1993, covering a wide range of latitudes from Ny Alesund, Norway to McMurdo, Antarctica [Melbourne, *et al.*]. Assuming a network of 30 ground receivers and a full GPS constellation, TEC can be simultaneously measured on approximately 240 lines-of-sight (8 at each ground site). Since the receivers are distributed around the globe, a large fraction of the "ionospheric shell" is sampled in just a few hours. Thus, such a network can ultimately provide the capability to make a "snapshot" of the global TEC distribution with few-hour or better temporal resolution, and a time series of such maps will reveal the evolution of the global TEC structure. Performing a global fit to data from many sites also allows one to bring much more data to bear on the problem of estimating the satellite instrumental biases. Since the ionospheric delay and the instrumental biases must be estimated simultaneously, we have found that the tasks of estimating the biases and modeling the ionosphere are intertwined and complementary. Currently, the uncertainty in the biases is the dominant error source in producing GPS-based TEC maps. Using multi-site fits instead of the older

single-site technique has led to improved bias values as evidenced by reduced day-to-day scatter in the bias estimates [see Wilson and Mannucci, 1993].

Local maps of TEC over single GPS receiver sites using GPS dual-frequency delays have been obtained previously by several groups including the authors [Royden, *et al.*, 1984; Lanyi and Roth, 1988; and Coco, *et al.*, 1991]. The method introduced by Lanyi and Roth assures that the electron distribution lies in a thin shell at a fixed height above the Earth, and the measured ionospheric delays are modeled by a two-dimensional polynomial function of shell angular position. In previous papers, we have extended this thin-spherical-shell fitting technique to multi-site GPS datasets using two-dimensional spherical (surface) harmonics as a global basis. Daily ionospheric maps of the northern hemisphere were produced for 23 days in Jan.-Feb. of 1991 and 11 days in Oct. of 1992 [Wilson, *et al.*, 1992 and Mannucci, *et al.*, 1992]. These maps were essentially a daily average ionosphere since each fit used 24 hours of GPS data. We are currently investigating several ways to improve the time resolution of the maps in order to fully exploit the potential of the global dataset [see Mannucci, *et al.*, 1993].

In this paper, the surface harmonic fitting technique has been used for periods as short as 12 hours. Due to limited ionospheric shell coverage, the time span cannot be reduced further with the harmonic fitting technique. The tradeoff between time resolution and shell coverage will be discussed below. A dataset consisting of 15 days of GPS data (Jan. 1-15, 1993) from 30 globally distributed sites in the IGS network has been investigated for this work. A world map showing the station locations appears in Figure 1. Note that only 5 of the sites are in the southern hemisphere, and that the northern hemisphere sites are confined to a latitude band from 2.5-80 degrees, except for the lone equatorial site at Kourou, French Guiana (KOUR). This dataset therefore has limited utility for studying the equatorial anomaly. However, the IGS network is growing rapidly (45 sites as of Nov. 1993) and

the geographic distribution of sites, particularly in South America and Africa, continues to improve with time,

Ionosphere Model and Estimation Technique

The thin spherical shell model is described in detail in Langley and Roth, 1988. Briefly, the vertical total electron content (TEC) is approximated by a spherical shell with infinitesimal thickness at a fixed height of 350 km above the Earth's surface. The shell is assumed to be time-independent in a reference frame fixed with respect to the Earth-Sun axis for several hours. The intersection of the line-of-sight from the receiver to the satellite with the spherical shell defines a "shell" latitude and longitude, where the zero of shell longitude points toward the Sun and the latitude, is defined relative to the Earth's equator. The line-of-sight TEC is assumed to be related to the vertical TEC by an elevation mapping function $M(\theta)$, which is the simple geometric slant ratio at the shell height h :

$$M(\theta) = \{1 - [\cos \theta / (1 + h/R)]^2\}^{-1/2}$$

where θ is the elevation angle and R is the radius of the earth. Dual-frequency GPS observations provide measurements of line-of-sight TEC, but are corrupted by instrumental delay biases between the L_1 and L_2 signal paths in the satellite transmitter and ground receiver. The instrumental bias can be measured directly for some ground receivers but the satellite transmitter biases must be estimated or obtained from an independent source. The line-of-sight differential delays for the i th receiver looking at the j th GPS satellite can be modeled by the following expression:

$$\tau^{LOS}_{ij} = \tau^r_i + \tau^s_j + K M(\theta_{ij}) TEC(\theta_{ij}, \phi_{ij})$$

where τ^{LOS}_{ij} is the line-of-sight differential delay, τ^r_i is the bias for the i th receiver, τ^s_j is the bias for the j th satellite transmitter, $K (= 2.85)$ is a constant relating differential delay

at 1. band in nanoseconds to ionospheric TEC in TECU, $M(1;ij)$ is the elevation mapping function, and $V(1;C)(\theta_{ij}, \phi_{ij})$ is the vertical TEC at shell latitude θ_{ij} and shell longitude ϕ_{ij} . The vertical TEC over the entire globe can then be fit to a surface harmonic expansion in θ and ϕ , while simultaneously estimating the receiver and satellite biases.

There is a tradeoff between shell coverage and temporal resolution when producing large-scale TEC maps from GPS data. To achieve adequate shell coverage given a limited number of ground sites and the geometry and angular velocity of the GPS satellites, a certain period of time must pass so that the line-of-sight from the ground site to the satellite can traverse a region of the ionospheric shell. However, the ionosphere is changing, during this period of time so the data span should be minimized in order to optimize the accuracy and temporal resolution of the maps. Figure 2 shows the shell coverage for data arcs of 24, 12, and 6 hours on Jan. 5, 1993. The longitudinal coverage for the 24 and 12 hour data arcs is adequate, but the coverage for the 6 hour data arc is too patchy in longitude to yield a reasonable surface harmonic fit. Note that for the 12-hour data arc the equatorial coverage spans only half of the longitude range since there is only one equatorial ground site (as of Jan. 1993).

The ionosphere model used is obviously a simplification. The notion of "mapping to vertical" makes sense only when horizontal TEC gradients are not too large. The assumption that the ionospheric shell height is constant everywhere is also an approximation. Simulations with Chapman profiles show that the functional form for the thin-shell mapping functions actually approximates the mapping function for distributed profiles as long as the height is chosen correctly [Hajj, 1993]. But choosing the incorrect height can lead to a biased estimation of vertical TEC along a satellite track.

Another limitation of this approach is the problematic assumption that the ionosphere is independent of time over several hours in the Sun-fixed reference frame. The ionosphere at

a fixed shell location will vary in time as a result of variations in the solar flux and other dynamics, such as traveling ionospheric disturbances. More importantly, a line of constant geomagnetic latitude varies in time by ± 11 degrees over 24 hours as expressed in the Sun-fixed longitude and geographic latitude coordinate system due to the offset between the magnetic and rotational poles of the Earth. Thus, the longer the span of data in a fit, the more one is averaging over magnetic-field-influenced variations in the ionosphere.

The accuracy of the ionospheric TEC maps obtained from GPS data is strongly affected by uncertainties in the satellite and receiver biases. These can be estimated independently along with the ionosphere since they do not share the same elevation angle dependence as the TEC. Because the elevation mapping function is only approximate and the ionosphere at a fixed shell location is changing during the time span of the fit, the ionosphere may be systematically mismodeled, leading to an improper separation of the elevation-dependent TEC from the elevation-independent biases. As a result, the bias estimates obtained from any one fit may be corrupted by ionospheric mismodeling. However, the biases are constant on a time scale of weeks to months, so better bias values can be obtained by averaging the estimates from many fits over 10-15 days. To further reduce the effects of ionospheric mismodeling, the estimation procedure can be applied using only nighttime data, when the ionosphere is relatively constant in time and therefore less susceptible to modeling errors. Nighttime data are defined to be those observations with ecliptic shell longitudes in the nighttime quadrant opposite the sun.

The following estimation strategy is used to produce the global maps. Each multi-site data arc is fit in a two-step process: first, the nighttime data alone are fit to determine receiver and satellite biases, and then, fixing the biases at average values obtained from nighttime fits performed over 10-15 days, the full daytime and nighttime dataset is used to estimate the global ionosphere. In both steps, the vertical TEC is modeled by 8th-order surface harmonics. Only TEC observations with elevation angles above 10 degrees have

been used in the fits. For a 2-minute data rate from 30 receivers, a full 12-hour fit consists of approximately 60,000 observations. Since the observable is sensitive only to the sum of the receiver and satellite biases, several of the receiver biases are constrained tightly (a priori standard deviation of 1 nanosecond) to values based on periodic receiver calibrations, while the rest of the receiver biases and all of the satellite biases are essentially unconstrained. This strategy allows one to determine absolute levels for the satellite and receiver biases, and it reduces sensitivity to a single erroneous receiver calibration.

Results

Multi-site fits of the GPS data from 30 IGS sites were performed for the period of Jan. 1-15, 1993. Since the majority of the sites are in the northern hemisphere, results are presented only for a limited latitude band of 20 to 80 degrees. A contour map of vertical f^oF_2 obtained from a 24-hour fit on Jan. 4, 1993 is shown in Figure 2. The f^oF_2 is expressed in the usual f^oF_2 units where $f^oF_2 \text{ (MHz)} = 10^{16} \text{ electrons/meter}^2$. Note the peak in the ionosphere just east of zero degrees longitude (the Sun axis) and the characteristic fall-off at nighttime. Figure 4 shows contour maps of three 12-hour fits covering the period of 00:00 UT on Jan. 4 to 12:00 UT on Jan. 5. These maps are representative of the thirty 12-hour maps produced for the 15 day period. The temporal evolution of ionospheric f^oF_2 can be investigated by examining a time series of global f^oF_2 maps. Using a false-color representation of f^oF_2 , a color ionosphere movie has been produced from the sequence of thirty 12-hour maps. The progressive change in the ionospheric structure over days to weeks is quite evident in the color movie.

To determine the accuracy of the harmonic fits, a map has also been made of the vertical residual ionosphere (observed f^oF_2 mapped to vertical minus the fit). Figure 5a shows a gray-scale map of the vertical root-mean-square ($\sqrt{\text{MS}}$) residuals for the 24-hour fit shown

in Figure 3. The **map** is formed by accumulating the RMS of the residuals into a one-by-one degree grid in latitude and longitude. White boxes represent grid squares for which there are no data as a satellite track never passed through that square. The residuals range from 0 to 20 TECU but most are in the range of 0 (light gray) to 10 (black) TECU. The total RMS of the residuals is 4.3 '1' TECU. Note that the residuals are below 5 TECU nearly everywhere in the 20-80 latitude band. Only in a localized region near 20 degrees latitude, where the coverage is sparse, do the residuals rise above 10 '1' TECU. The vertical RMS residuals for the 12-hour map in figure 4a are shown in figure 5b. The total RMS of these residuals is 2.1 TECU. Note that the residuals for the 12-hour map are smaller than those for the 24-hour map, as expected since for the 12-hour fits there is less time-averaging than for the 24-hour fits. For the 24-hour fit, there can be two observations at the same shell position separated by nearly 24 hours. If the ionosphere has changed substantially, the two observations will not be consistent and the fit cannot match both of them, resulting in a large residual. This effect may also account for the large residuals in the lower latitude region of the map, since in this region variations due to the magnetic pole rotation are expected to be largest.

Another way to check the robustness of the estimation strategy is to remove one or more sites from the dataset, perform a fit with the remaining sites, and then calculate the vertical residuals for the observations at the removed sites. The result is a measure of how well the maps predict the TEC at shell locations where there are no data. Figure 6 shows a plot of the Usuda vertical residuals versus shell longitude for a 24-hour fit on Jan. 5 excluding the Usuda data. Except for a few GPS tracks near the Sun axis, the residuals are below 5 TECU in magnitude. The residuals are essentially unchanged when the data from Usuda are added to the fit. The RMS of the residuals without Usuda data is 2.8 TECU; with Usuda data it is 2.6 TECU. This striking result illustrates both the benefits and problematic aspects of 12 or 24-hour surface harmonic fits. Using a long span of data and fitting the data on a Sun-fixed shell effectively spreads the longitudinal coverage, so the '1'11~ above

Usuda can be estimated by using data from sites which cover Usuda's latitude band but are remote in longitude. Thus, using harmonic fits to produce global maps gives one the capability to predict the vertical TEC at a site with no GPS receiver (or no data that day) by using GPS data from remote sites. However, near the Sun axis where the ionosphere is large and can exhibit large temporal fluctuations, the temporal-averaging inherent in the fits may lead to large errors. We anticipate that the harmonic fitting strategy will be more effective in the mid-latitude regions where the ionosphere is better behaved (fewer large temporal fluctuations) than in the equatorial and auroral regions.

To investigate the accuracy of the remote calibration capability, one can look at the vertical TEC above a site during a 24-hour period, as predicted by a global map which does not include GPS data from that site. This prediction can then be compared to estimates obtained from single-site and global fits that do use the data from that site. Figure 7a plots the vertical TEC directly above the Goldstone (GOLD on figure 1) receiver site versus time for the 24 hours of Jan. 5 as predicted by five different fits: (1) a single-site fit of Goldstone data, (2) a 24-hour global fit including the Goldstone data, (3) a 24-hour global fit excluding the Goldstone data, (4) a pair of 12-hour global fits including the Goldstone data, and (5) a pair of 12-hour global fits excluding the Goldstone data. The five predictions agree to a few TEC units. Figure 7b shows a similar plot of the five predictions for the TEC above the Usuda site. The Usuda site is more isolated than the Goldstone site, but for the 24-hour global fits the agreement with the single-site fit is still quite good since Usuda's latitude band is well covered by other sites.

The effect of choosing an incorrect elevation mapping function has been investigated by performing the estimation procedure with a different elevation angle cutoff. Two 24-hour maps were made using 10 and 20-degree elevation angle cutoffs. The difference map shown in Figure 8 was formed by differencing two one-by-one degree grids. The difference grid points have a mean of -0.14 TECU and a standard deviation of 0.85

THICU. The map has been restricted in latitude range to 30-80 degrees since the larger elevation cutoff reduces the coverage in the latitude range of 20-30 degrees. Note that the difference varies smoothly between positive and negative values. This could correspond to a smoothly varying error in shell height over the given regions. For both maps, a constant shell height of 350 km is assumed. If the "effective" shell height is larger (smaller) than 350 km, then mapping errors at low elevation will cause the ionosphere to be underestimated (overestimated).

Conclusions

A world-wide network of GPS receivers provides a unique opportunity to continuously monitor the ionosphere on a global scale. While the IGS network had severely limited equatorial and southern hemisphere coverage as of 1992, approximately 15 receiver sites were added in 1993 and more will come on-line in the near future. Larger, more uniformly distributed networks will provide denser longitudinal coverage for shorter data arcs, enabling ionospheric mapping with hourly or sub-hourly temporal resolutions. Since the IGS network is permanent and continuously operating, hourly global ionospheric maps could be produced continuously.

We have produced global THIC maps every 2 hours for 15 days in Jan. 1993 by fitting vertical THIC measurements from 30 GPS receiver sites to a two-dimensional spherical harmonics basis. Since the majority of the receiver sites are in the northern hemisphere for this dataset, the maps are only useful for the latitude band of 20-80 degrees in the northern hemisphere. The RMS of the fit residuals is less than 3 THICU for that latitude band. By fitting the data on a Sun-fixed shell, we have developed a rough capability to predict the ionosphere at an isolated site using GPS data from other sites in the same latitude band. Preliminary results indicate that, for sites in the mid-latitudes, the global maps are able to

predict the diurnal curve of vertical TEC over a site to within 5 TECU. Further study and comparisons of 10 independent ionosphere measurements will be required to verify the accuracy of the global maps.

The surface harmonic fitting technique used in this analysis limits the maps to a time resolution of 12 hours or longer. Efforts are under way to improve the time resolution by using a better set of basis functions. A disadvantage of surface harmonics is that they are non-zero over the entire sphere; they have "global support". For investigating ionospheric behavior on time scales much shorter than 12 hours, it will be necessary to use basis functions with "local support", that is basis functions which are non-zero only over a limited area of the shell. We are developing a triangular interpolation technique in which the ionospheric shell is tiled with triangles and the TEC at each vertex is estimated by local interpolation of the TEC data within the triangles. The TEC at each vertex is treated as a stochastic parameter (random walk) and is updated every hour [Mannucci, *et al.*, 1993]. Using the local triangular basis with a stochastic estimation strategy should produce more accurate maps when coverage is sparse.

As we gain more experience with mapping techniques, we anticipate that a more physics-based parameterization of the ionosphere will be required to accurately model the high-latitude and equatorial ionospheres. The physics of the three ionospheric regions- equatorial, mid-latitude, and auroral- is quite distinct. In regions where data coverage is sparse, *a priori* information from a semi-empirical ionosphere model which incorporates the relevant ionospheric physics (e.g., the Bent [Bent, *et al.*, 1976] or PRISM models [Anderson, 1993]) could be used to bridge the gaps in the data.

Acknowledgments. This analysis was made possible by the high quality of the IGS dataset, the result of a collaborative effort involving many people at JPL and at other centers around the world.

We also wish to express our appreciation to George Hajj, Dave Imel, and Herb Royden for helpful

discussions and suggestions. The research described in this paper was performed by the Jet Propulsion Laboratory, California Institute of Technology, under contract with the National Aeronautics and Space Administration.

References

- Anderson, D. N. (1993) The development of global semi-empirical ionospheric specification models, *Proceedings of the Seventh International Ionospheric Effects Symposium*, J. Goodman, ed., Alexandria, VA, May 1993.
- Bent, R. B., S. K. Jewell, G. Nesterzuk, and P. H. Schmid (1976), The development of a highly successful worldwide empirical ionospheric model, in J. Goodman (Ed.), *Effect of the Ionosphere on Space Systems and Communications*, Springfield, VA: National Technical Information Service, 1976, 13-28.
- Coco, D. S., C. E. Coker, S. R. Dahlke, and J. R. Clynch (1991), Variability of GPS Satellite Differential Group Delay Biases, *IEEE Transactions on Aerospace and Electronic Systems*, **27** (6), 931-938.
- Hajj, G., private communication, March, 1993.
- Lanyi, G. and '1', Roth (1988), A comparison of mapped and measured total ionospheric electron content using global positioning system and beacon satellite observations, *Radio Sci.*, **23** (4), 483-492.

Mannucci, A. J., 11.11, Wilson, and C. D. Edwards (1992.), Global Maps of Ionospheric Total Electron Content Using the IGS GPS Network, poster presented at the AGU Fall Meeting, San Francisco, December, 1992.

Mannucci, A. J., B. D. Wilson, and C. D. Edwards (1993) A New Method for Monitoring the Earth's Ionospheric Total Electron Content using the GPS Global Network, to appear in *Proceedings of the Institute of Navigation GPS-93*, Salt Lake City, Utah, September, 1993.

Melbourne, W. G., S. S. Fisher, R. E. Neilan, P. P. Yunck, B. Eingen, C. Reigber, and S. Tatavjan (1991), The First GPS IERS and Geodynamics Experiment- 1991, IUGG/IAG Symposium, Vienna, August, 1991, Springer-Verlag, NY.

Royden, H. N., R. B. Miller, and L. A. Buenmigel (1991), Comparison of NAVSTAR satellite L-band ionospheric calibrations with Faraday rotation measurements, *Radio Sci.*, **19**, 798-800.

Wilson, B. D., A. J. Mannucci, and C. D. Edwards (1992), Global Ionospheric Maps Using a Global Network of GPS Receivers, Beacon Satellite Symposium, Cambridge, MA, July, 1992.

Wilson, B. D. and A. J. Mannucci (1993) Instrumental biases in ionospheric measurements derived from GPS data, to appear in *Proceedings Of Institute of Navigation GPS-93*, Salt Lake City, Utah, September, 1993.

(The figures will, of course, be reduced and laid out differently.
The figure captions for multiple part figures have been
repeated on each page for convenience.)

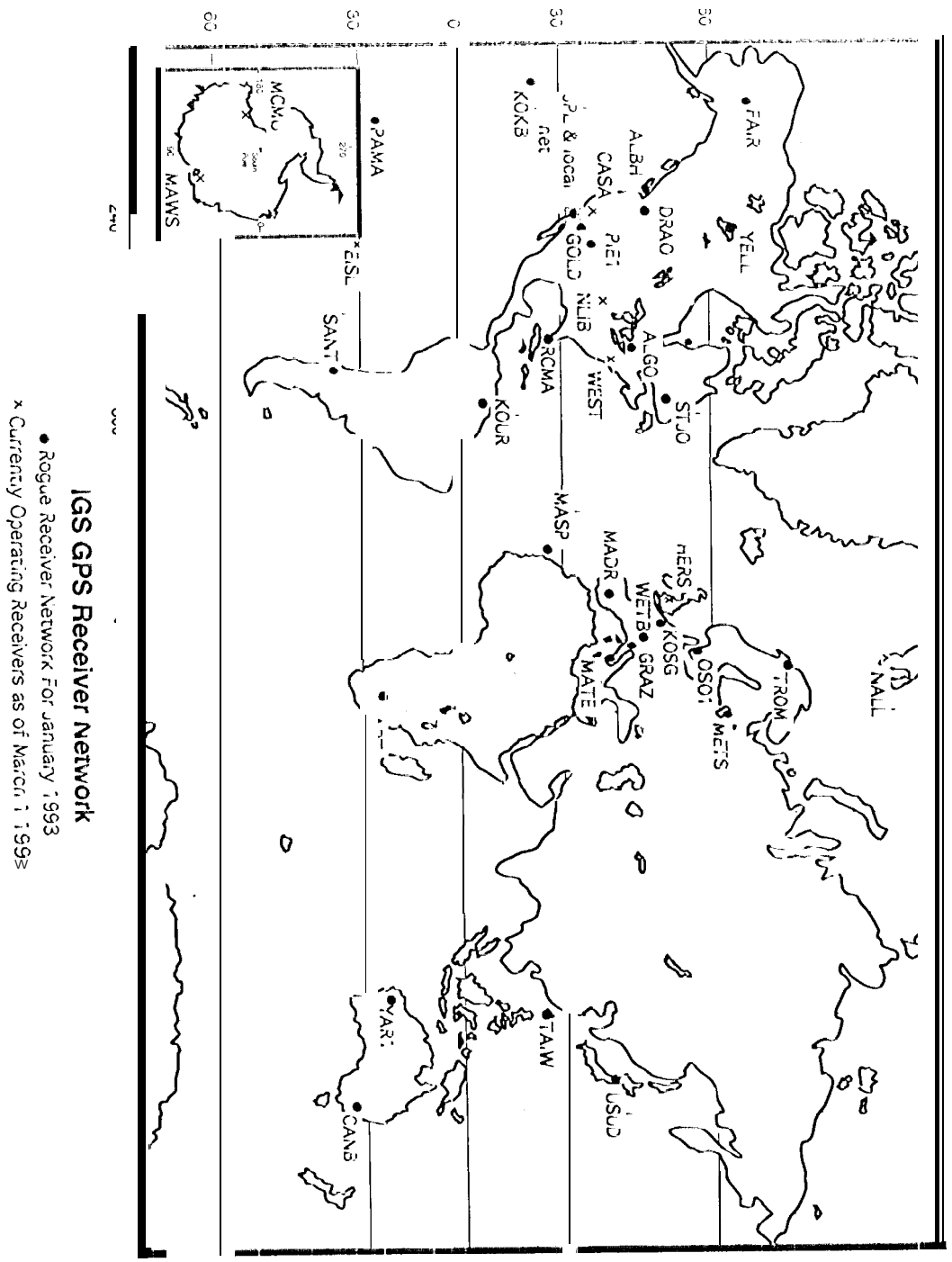


Figure — This map shows the receiver locations for the International GPS Service. The receivers at the locations denoted by a filled circle provided the data used in this paper. Additional locations that became available as of March 1, 1993 are denoted by an X-mark.

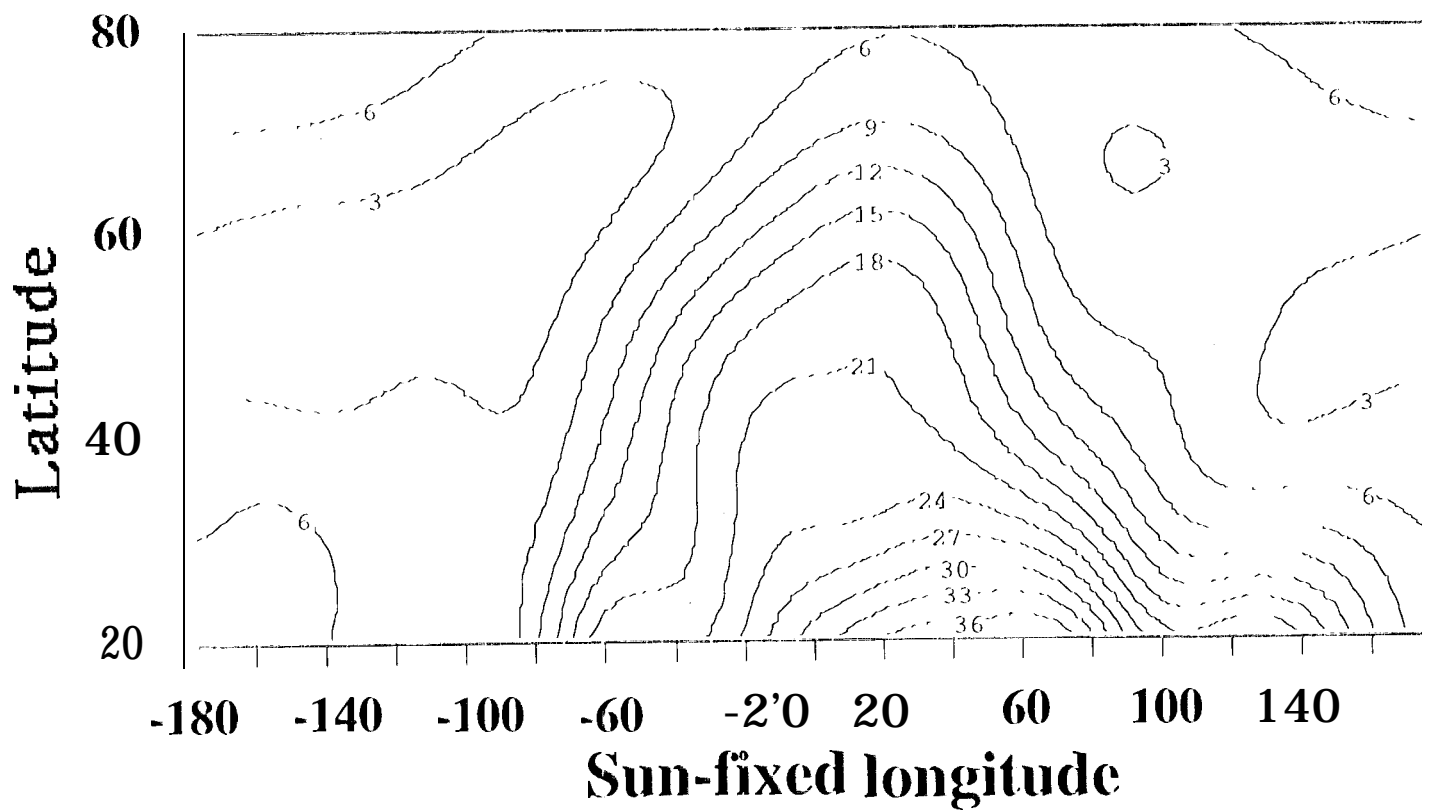


Figure 2, . . . - Global ionospheric TEC distribution for January 4, 1993 derived from a 24-hour fit. Contours are labeled in units of 10^{16} el/m².

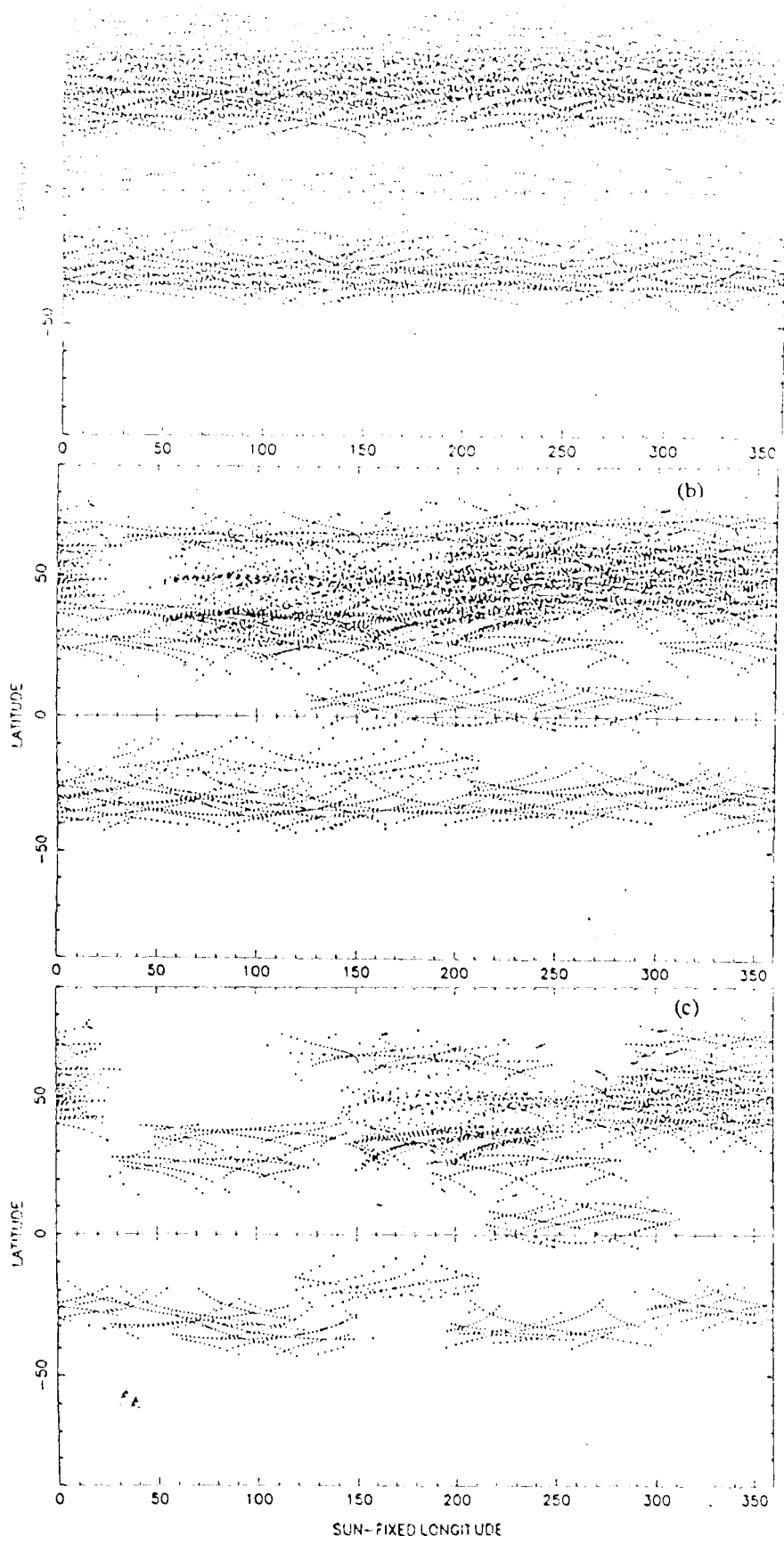


Figure 3. Fig. 2 shows "coverage plots" for the receiver network of Fig. 1 (filled circles only) for three time intervals on January 5, 1993. A point is plotted for each shell intercept point made between a receiver and transmitter. The standard "sun-fixed" co-ordinate system is used for these plots: 0 degrees longitude is the Sun-Larth direction and the Earth rotates underneath. The latitude of this system is the same as geographic. Fig. 3a which covers the period 00:00-24:00 UT on January 5. A single receiver in the equatorial region (Kourou, French Guyana) provides sparse coverage there. In Fig. 3b, the shell coverage for the period 00:00-12:00 UT is shown. In Fig. 3c the coverage for the 6-hour period of 06:00-12:00 UT is shown.

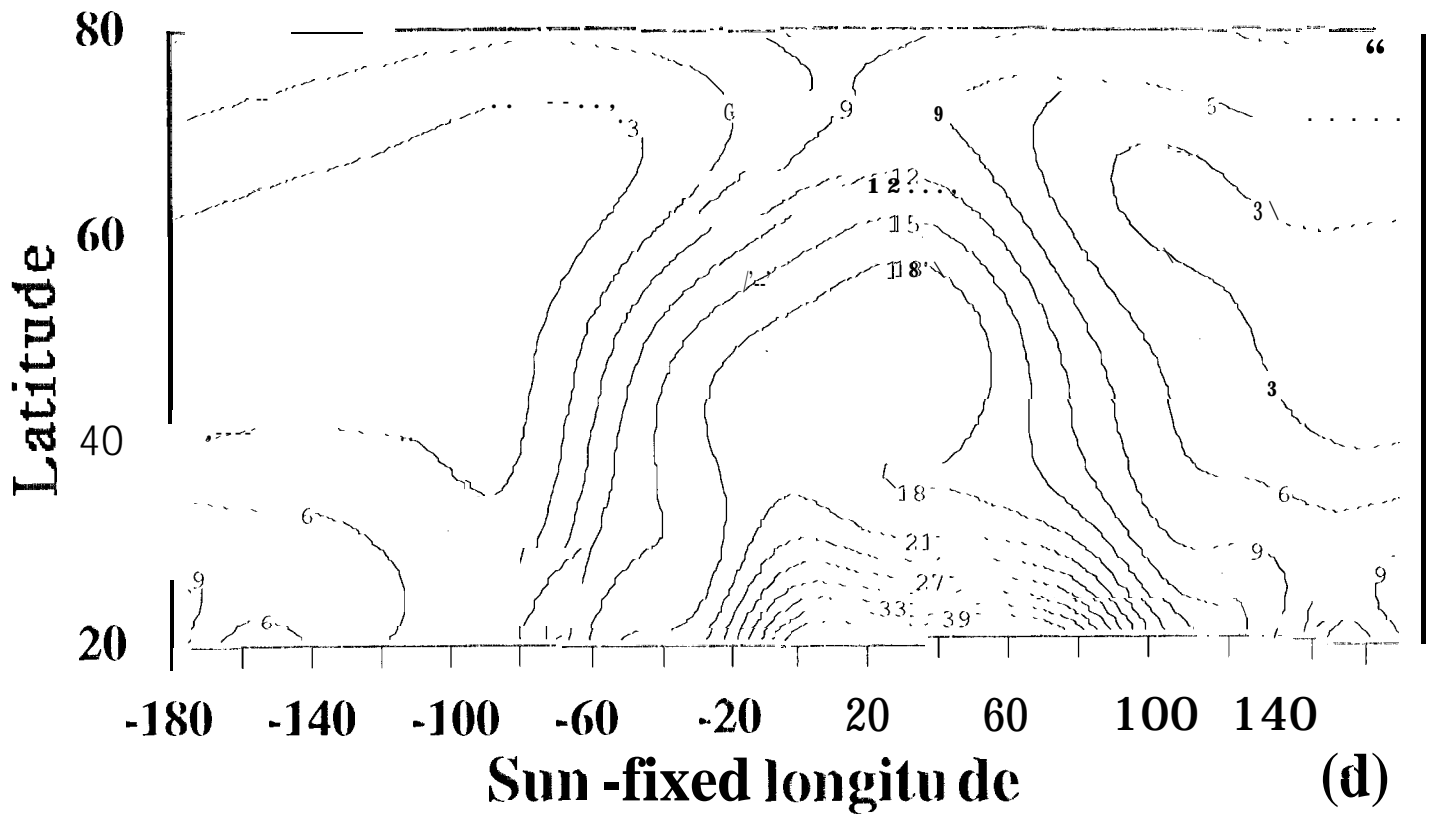


Figure 4-. Global ionospheric TEC distribution for January 4-5, 1993 derived from three 12-hour fits. Contours are labeled in units of 10^{16} el/m². (a) Fit of data from 0-1211'J' on Jan. 4. (b) Fit of data from 12-24 UT on Jan4. (c) Fit of data from 0-12 UT on Jan 5.

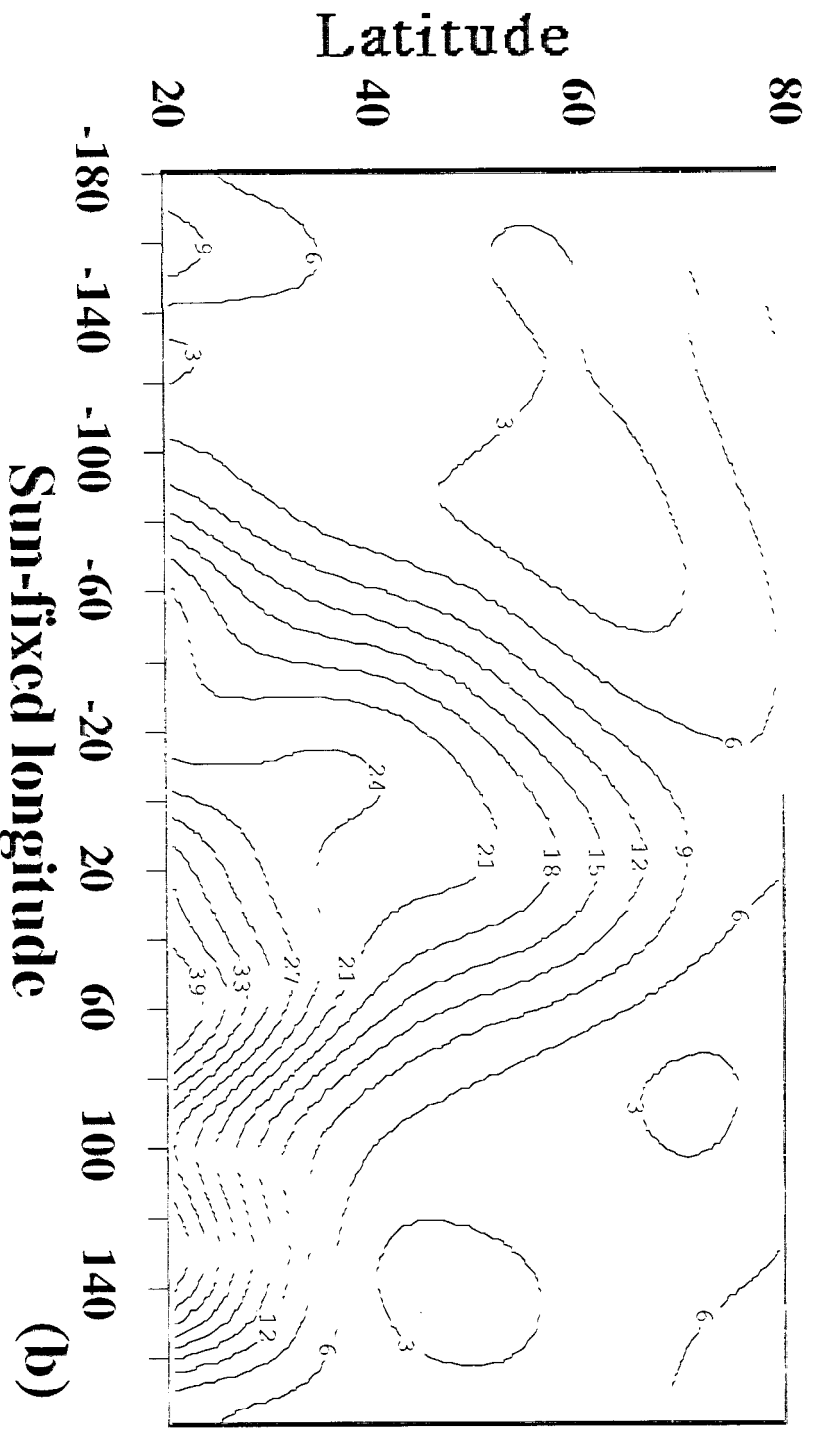


Figure 4 - Global ionospheric TEC distribution for January 4-5, 1993 derived from three 12-hour fits. Contours are labeled in units of 10^{16} e/m². (a) Fit of data from 0-12 UT on Jan. 4. (b) Fit of data from 12-24 UT on Jan.4. (c) Fit of data from 0-12 UT on Jan 5.

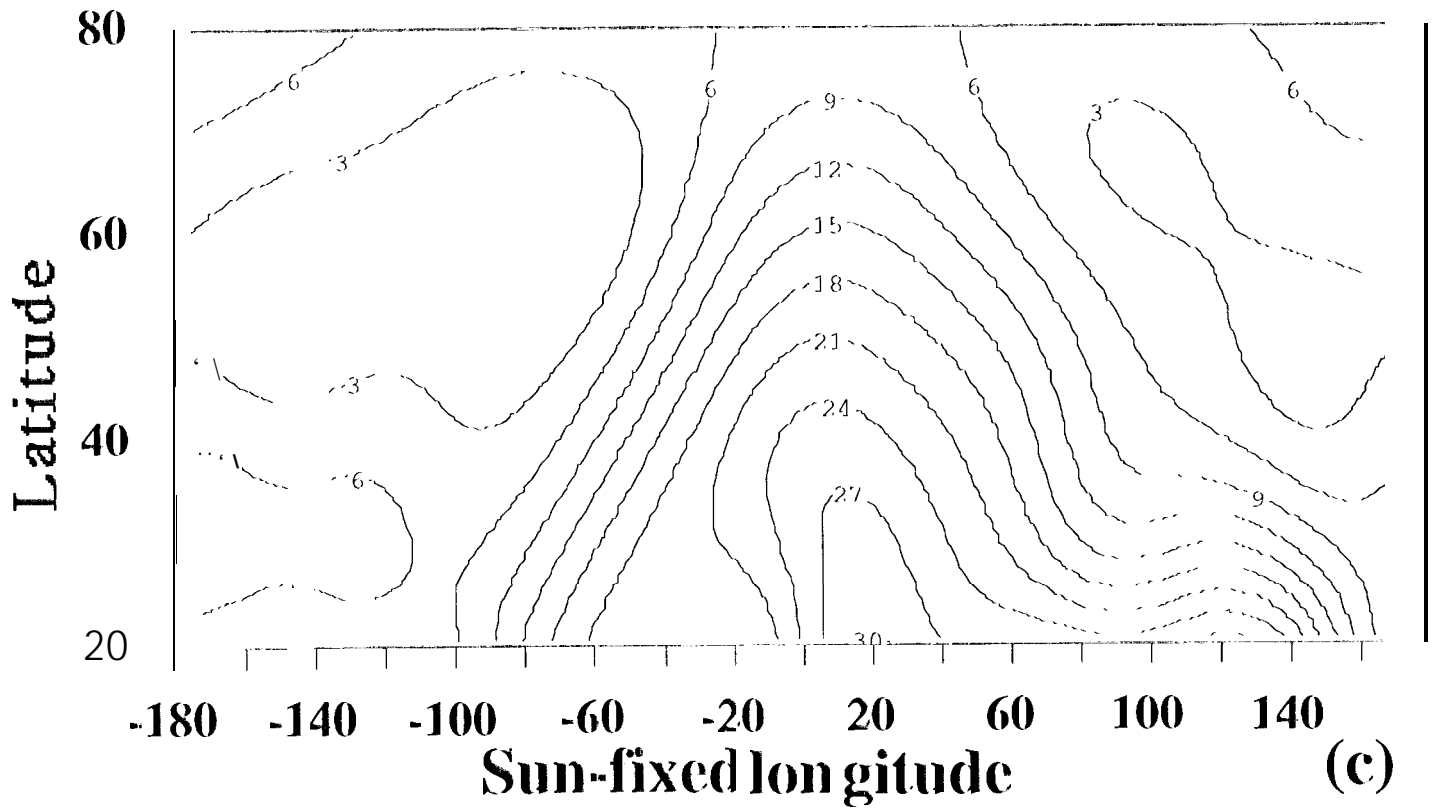


Figure 4 -- Global ionospheric TEC distribution for January 4-5, 1993 derived from three 12-hour fits. Contours are labeled in units of 10^{16} el/m². (a) Fit of data from 0-12 UT on Jan. 4. (b) Fit of data from 12-24 UT on Jan 4. (c) Fit of data from 0-12 UT on Jan 5.

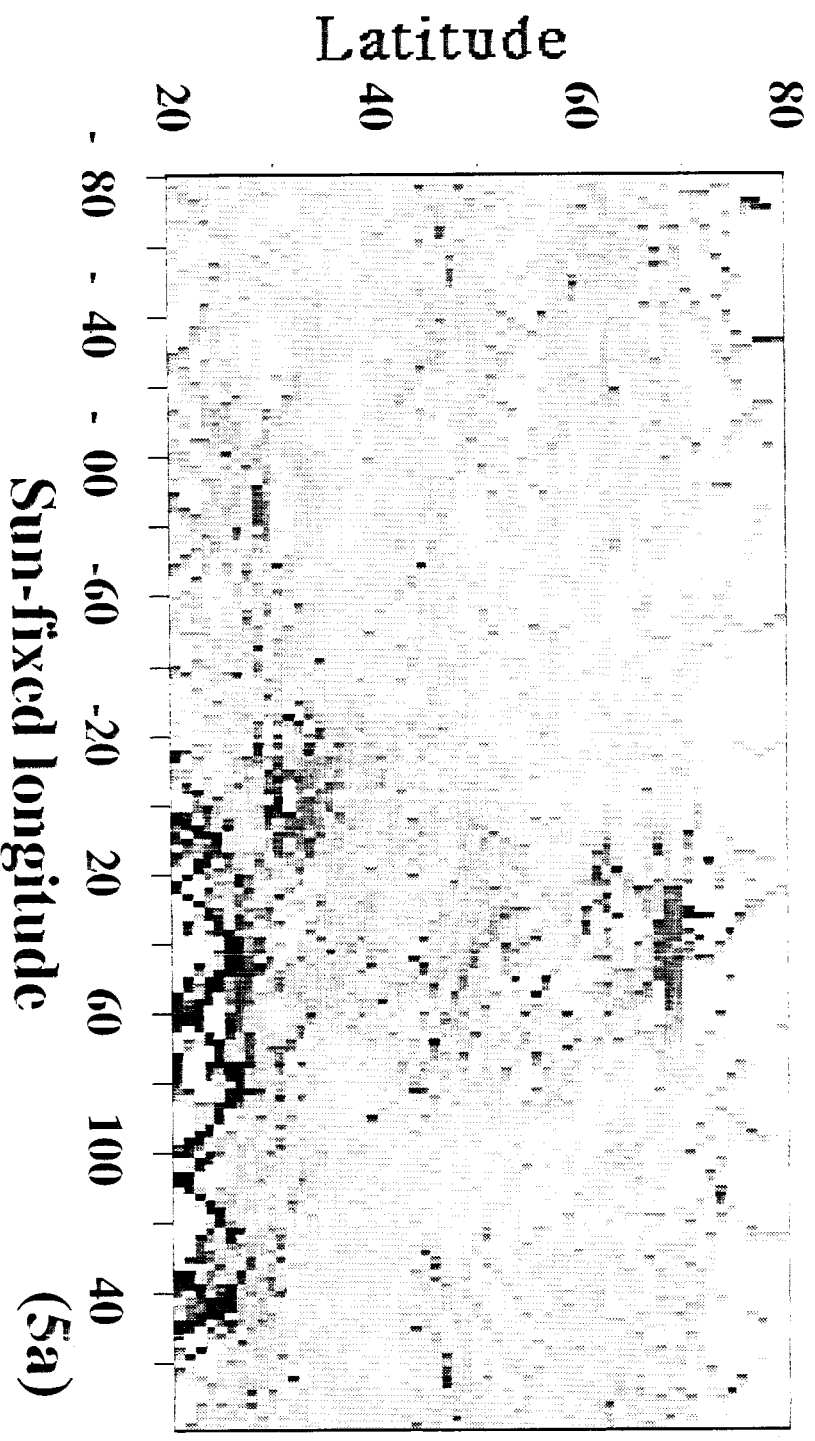


Figure 5 - Gray-scale map of fit residuals on Jan. 4, 1993. RMS residuals were accumulated into a one-by-one degree grid. White boxes are regions without coverage. The range is from 0 (light gray) to 10 TRFCU (black). (a) Residuals for a 24-hour fit. (Total RMS = 4.3 TRFCU). (b) Residuals for a 12-hour fit using data from 0-12 UT (Total RMS = 2.1 TRFCU).

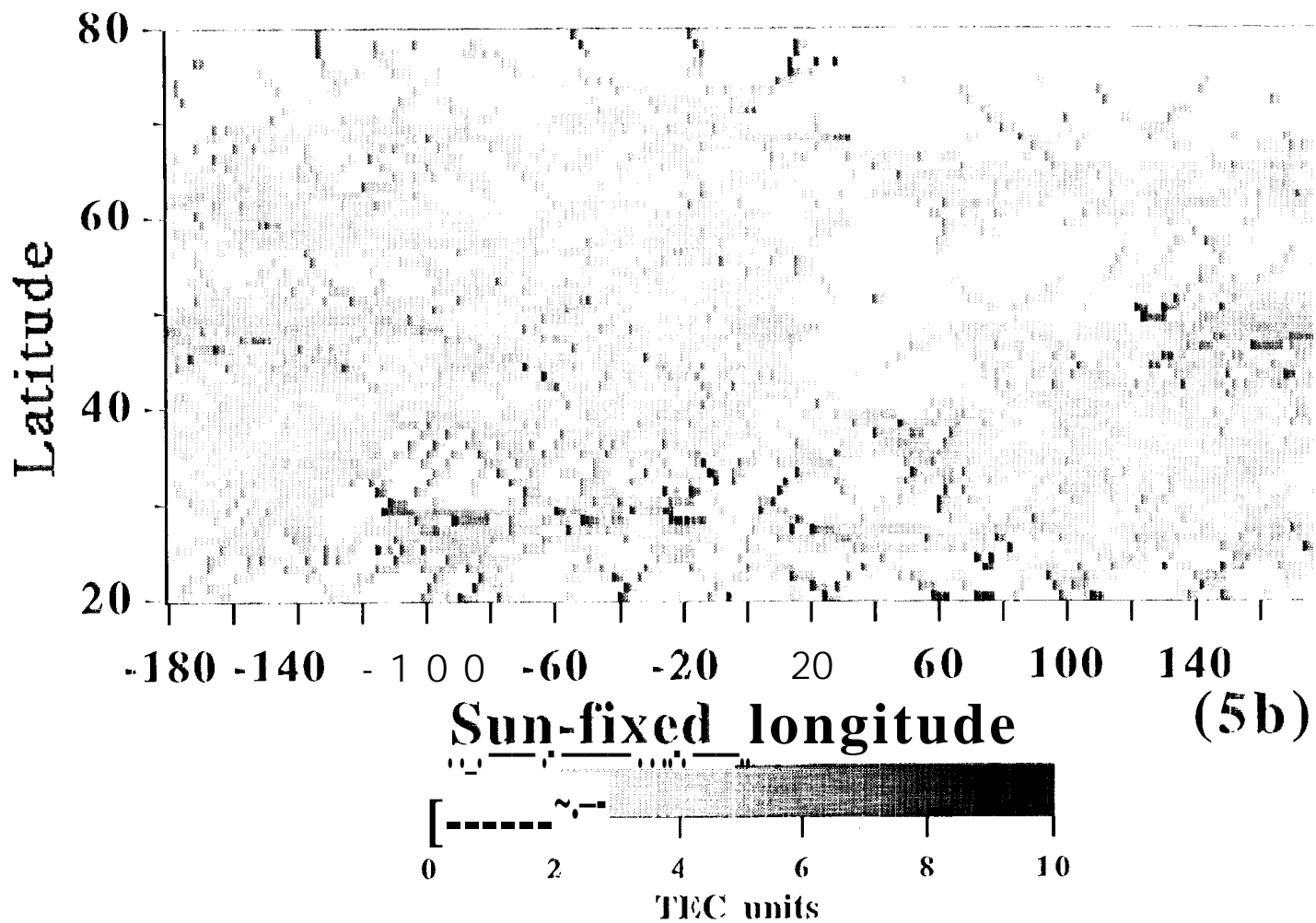


Figure 5 — Grq-scale map of fit residuals on Jan. 4, 1993. RMS residuals were accumulated into a one-by-one degree grid. White boxes are regions without coverage. The range is from 0 (light gray) to 10 TECU (black). (a) Residuals for a 24-hour fit (Total RMS = 4.3 TECU). (b) Residuals for a 12-hour fit using data from 0-12 UT (Total RMS = 2.1 TECU).

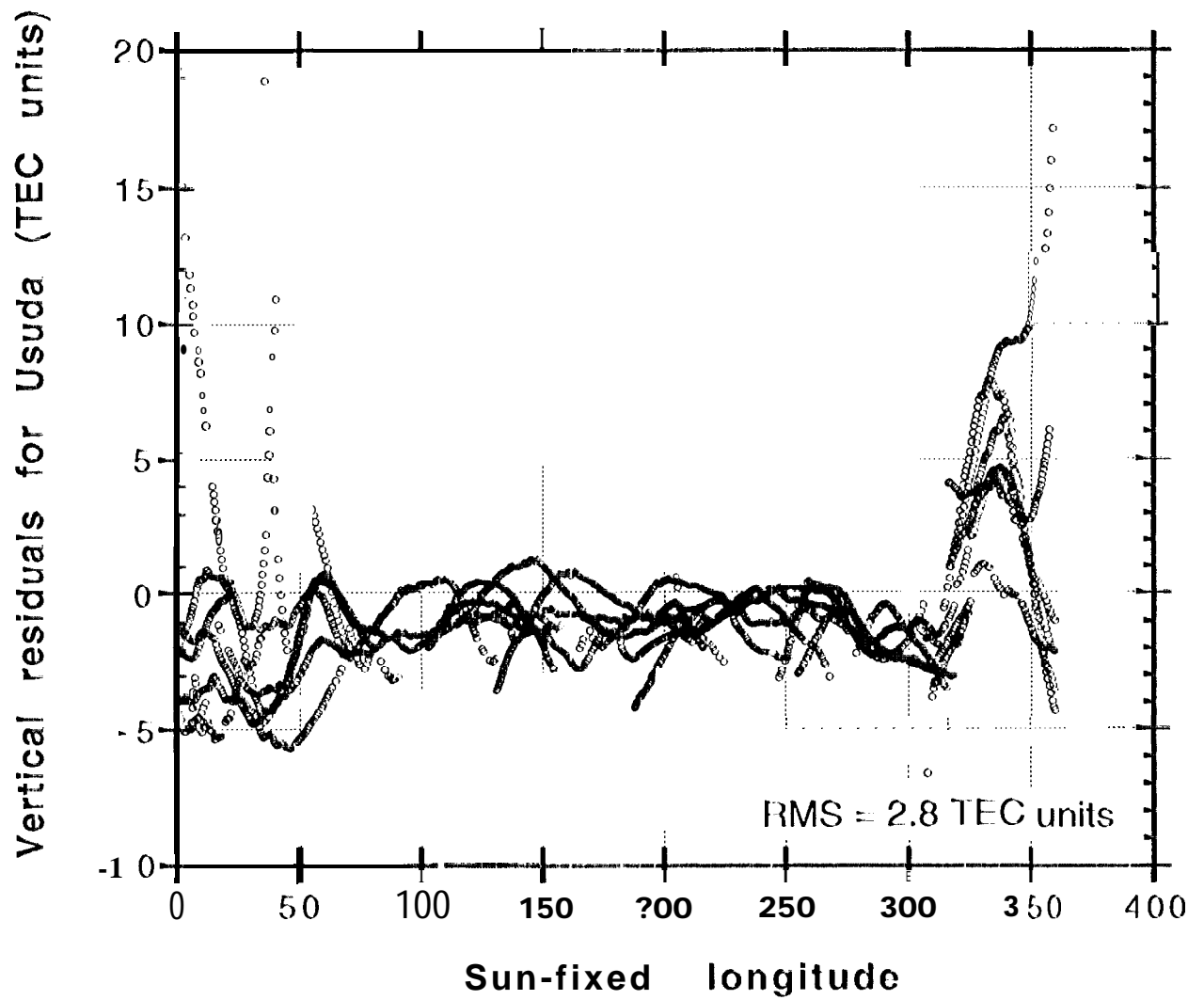


Figure 6 - Vertical residuals (observed mapped to vertical minus the fit) for the Usuda site on 93/01/08. The fit is a 24-hour fit excluding the Usuda data. The Sun is at zero degrees longitude.

24-hr global with Goldstone	12-hr global without Goldstone
- 24-hr global without Goldstone	Goldstone single-site
12-hr global with Goldstone	

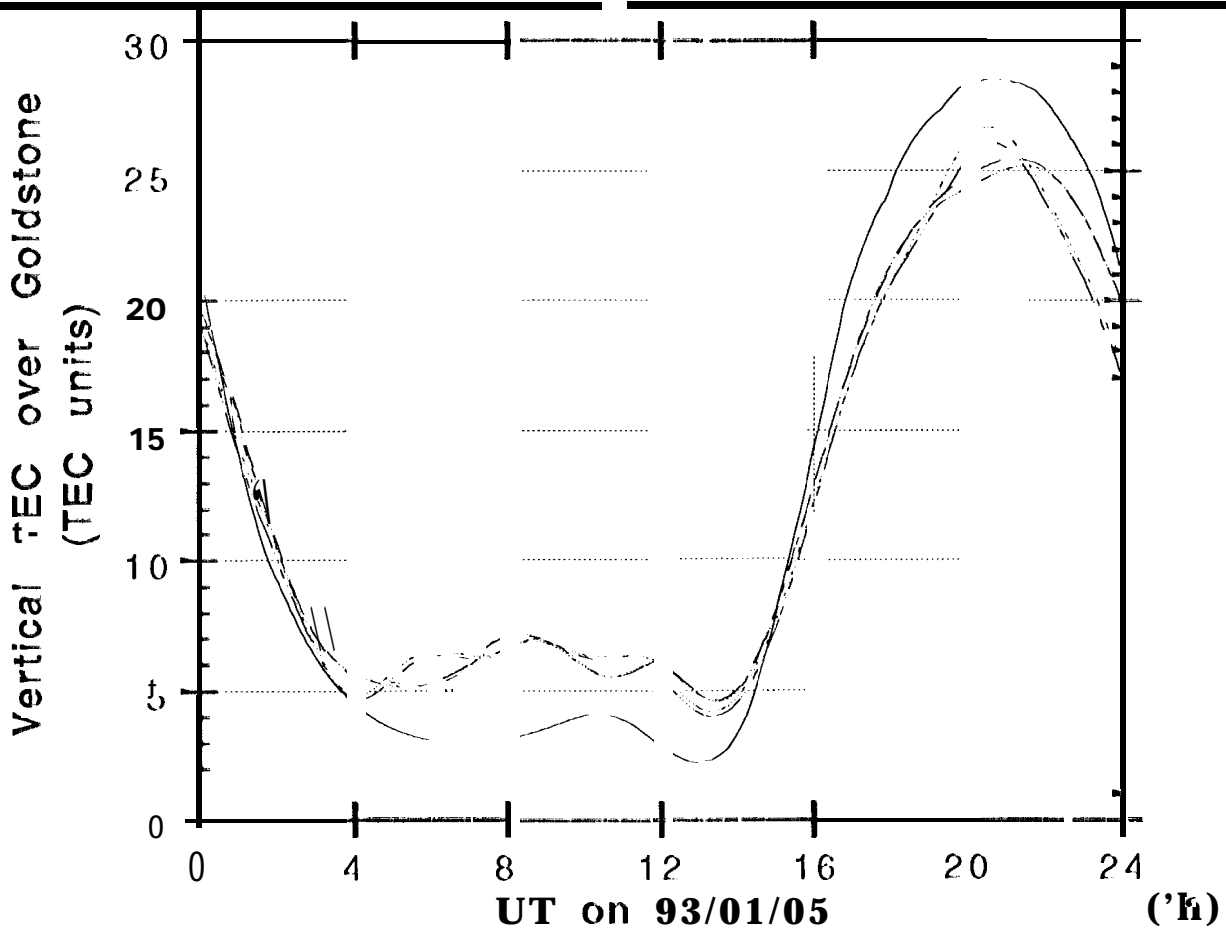


Figure 7 --- Vertical TEC directly above (a) Goldstone and (b) Usuda during the 24 hours of Jan. 5 as predicted by five different fits. The solid line is the single-site fit and the rest are global fits. Notice that the global fits excluding the chosen site are within a few TEC units of the single-site fit.

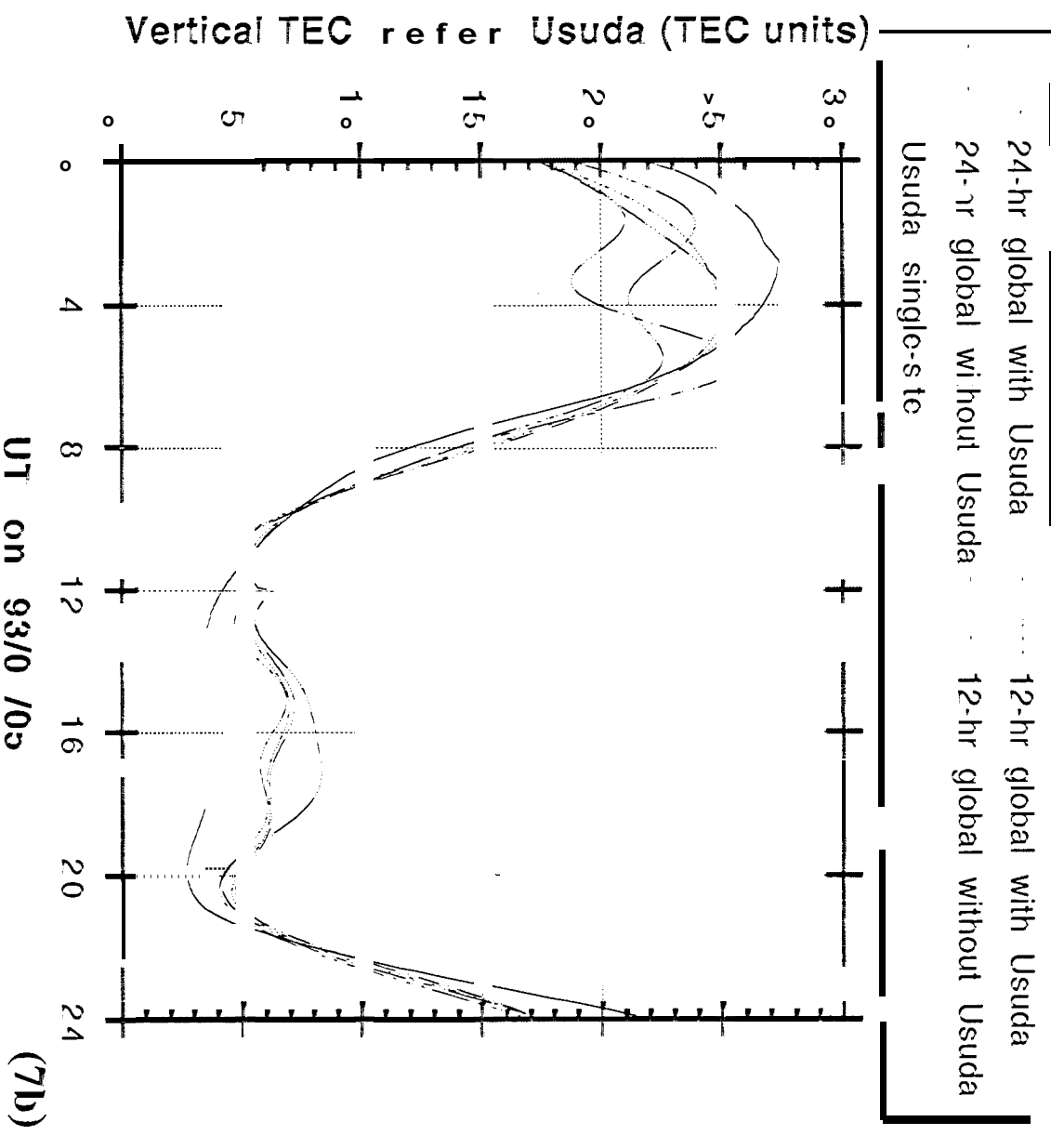


Figure 7 - Vertical TEC directly above (a) Goldstone and (b) Usuda during the 24 hours of Jan. 5 as predicted by five different fits. The solid line is the single-site fit and the rest are global fits. Notice that the global fits excluding the chosen site are within a few TEC units of the single-site fit.

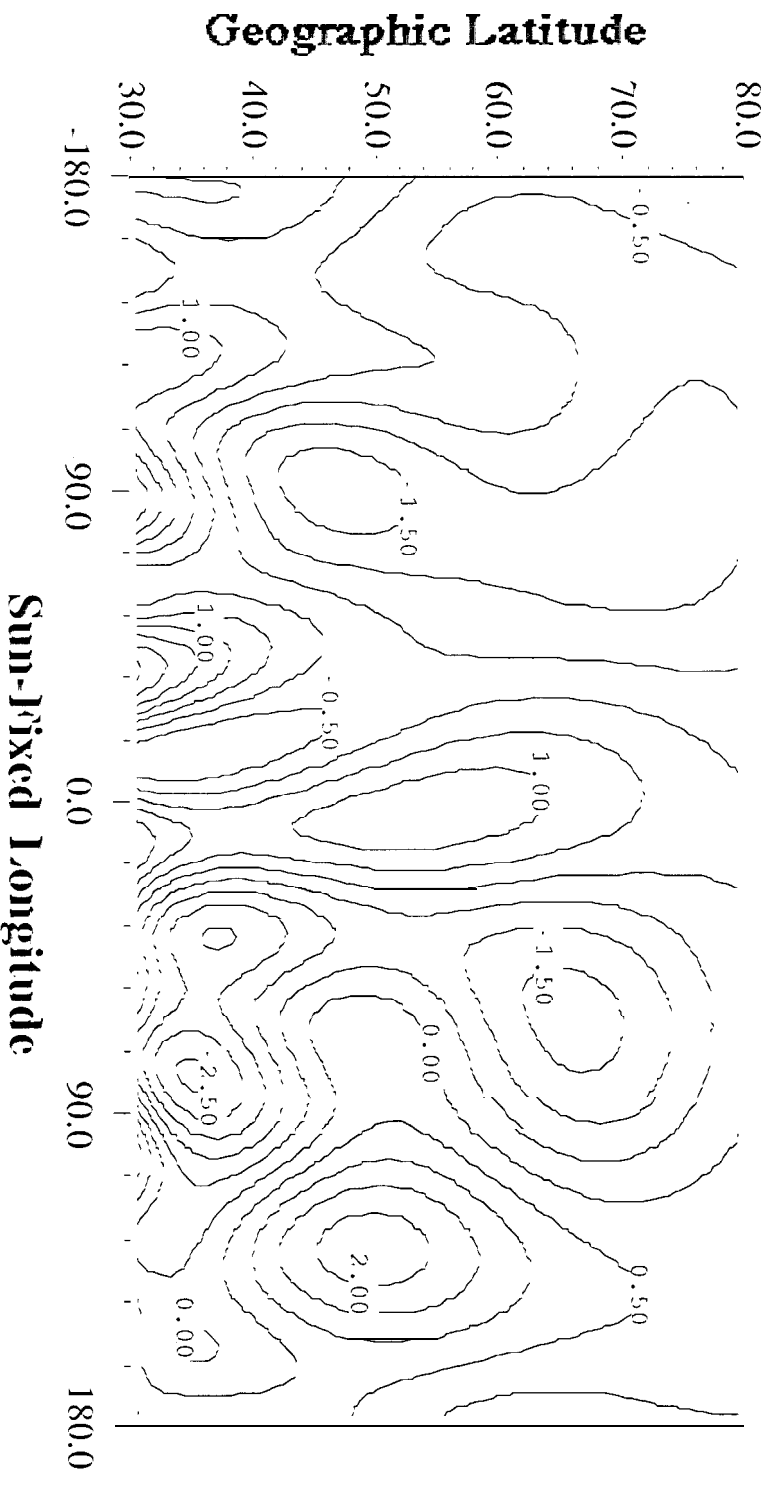


Figure 8

The difference of two 24-hour TWC maps which differ in elevation angle cutoff: 20 degrees versus 10 degrees. The difference map is formed by differencing two one-by-one degree grids. Notice that the differences are small and nearly zero mean which indicates that including data down to 10 degrees is not significantly altering the maps.